



Published in final edited form as:

Brain Struct Funct. 2017 August ; 222(6): 2759–2771. doi:10.1007/s00429-017-1370-x.

Microglia in the primate macula: Specializations in microglial distribution and morphology with retinal position and with aging

Janani Singaravelu¹, Lian Zhao¹, Robert N. Fariss², T. Michael Nork³, and Wai T. Wong¹

¹Unit on Neuron-Glia Interactions in Retinal Disease, National Eye Institute, National Institutes of Health, Bethesda, MD 20892, USA

²Biological Imaging Core, National Eye Institute, National Institutes of Health, Bethesda, MD 20892, USA

³Department of Ophthalmology and Visual Sciences, University of Wisconsin-Madison, Madison, WI 53792, USA

Abstract

Microglia, the principal resident immune cell in the retina, play constitutive roles in immune surveillance and synapse maintenance, and are also associated with retinal disease, including those occurring in the macula. Perspectives on retinal microglia function have derived largely from rodent models and how these relate to the macula-bearing primate retina is unclear. In this study, we examined microglial distribution and cellular morphology in the adult rhesus macaque retina, and performed comparative characterizations in three retinal locations along the center-to-periphery axis (parafoveal, macular, and the peripheral retina). We found that microglia density peaked in the parafoveal retina and decreased in the peripheral retina. Individual microglial morphology reflected macular specialization, with macular microglia demonstrating the largest and most complex dendritic arbors relative to other retinal locations. Comparing retinal microglia between young and middle-aged animals, microglial density increased in the macular, but not in the peripheral, retina with age, while microglial morphology across all locations remained relatively unchanged. Our findings indicate that microglial distribution and morphology demonstrate regional specialization in the retina, correlating with gradients of other retinal cell types. As microglia are innate immune cells implicated in age-related macular diseases, age-related microglial changes may be related to the increased vulnerability of the aged macula to immune-related neurodegeneration.

Keywords

Microglia; retina; macula; aging; primate; cellular morphology

Contact: Wai T. Wong, Unit on Neuron-Glia Interactions in Retinal Disease, Building 6, Room 215, National Eye Institute, National Institutes of Health, Bethesda, MD 20892, USA. Tel: +1 301 496 1758; fax: +1 301 496 1759; wongw@nei.nih.gov.

Author contributions

JS, LZ, RNF, and WTW planned the experiments, JS and LZ conducted the experiments, TMN prepared materials for the experiments, JS and WTW wrote the manuscript. All authors reviewed the manuscript and provided critical comment.

Competing Financial Interests

None of the authors have no conflicts of interest, financial or personal, to disclose.

Introduction

Microglial cells constitute the principal resident innate immune cell in the central nervous system (CNS) and have been implicated in various functional and pathogenic roles across an animal's lifespan from early development to late senescence (Tay et al. 2016). In addition to performing immune functions, microglia play important roles in guiding normal neuronal development (Frost and Schafer 2016) and maintaining the healthy physiological function of the adult CNS (Eyo and Wu 2013). In pathological situations, microglia, either from a loss of endogenous function or from the acquisition of inappropriate functions, are thought to contribute to the onset and/or the progression of CNS disease, particularly in the aged CNS (Perry and Holmes 2014; von Bernhardi et al. 2015). From these associations, microglia have been proposed as candidate cellular targets for therapeutic intervention for neurodegenerative diseases (McGeer and McGeer 2015).

In the retina, microglia have similarly been implicated as playing significant roles in preserving constitutive retinal function under healthy conditions (Wang et al. 2016; Li et al. 2015), as well as contributing to the progression of retinal disease in pathological conditions (Karlstetter et al. 2015). In the healthy adult retina, microglia are present as horizontally ramified cells that have a tiled distribution in the inner retina and with their processes concentrated in the inner and outer plexiform layers (Boycott and Hopkins 1981; Vrabec 1970). These microglial processes demonstrate rapid, constitutive, surveying movements in the retina (Lee et al. 2008) which have been implicated in functions of immune surveillance and synapse maintenance (Hristovska and Pascual 2015). In retinal injury and disease, microglia demonstrate overt migrations towards sites of injury (Ng and Streilein 2001; Thanos 1992), interacting with other retinal neurons and glia to influence the overall disease outcome (Zhao et al. 2015). These microglial phenotypes in health and disease have been found to change significantly with aging (Damani et al. 2011; Ma et al. 2013), indicating that aging changes in microglia may contribute to age-related retinal diseases (Ma and Wong 2016). Consistent with these observations, microglia can be localized to sites of pathology in a number of inflammatory and degenerative retinal diseases, including macular diseases with an aging component such as age-related macular degeneration (AMD) and diabetic macular edema (Madeira et al. 2015).

As studies on retinal microglia have been in large part performed in rodent models lacking a macula, less is directly known about how retinal microglia participate in macular diseases. How microglial cells are distributed and organized in the primate macula and whether these cells demonstrate particular specializations depending on their spatial position in the retina have not been addressed in detail. Characterization of these features can shed light on microglial functions in the specialized region of the macula and provide insight into how microglial dysfunction in the macula can participate in macular disorders. The question of whether and how microglia in the macula change with aging can also relate to how the aging macula becomes more vulnerable to degenerative processes.

In the current study, we performed a detailed and quantitative characterization of microglia in rhesus macaque (*Macaca mulatta*) retina. We investigated and compared how microglia varied in their distributions in separate retinal layers as a function of retinal position in the

foveal region, the outer macular region and the peripheral retina. Using quantitative 3-dimensional morphometric analyses, we examined whether graded alterations in microglial morphology exist in separate retinal loci ranging from the foveal region to the peripheral retina. To elucidate how these microglial specializations may undergo change in the aging macula, we performed comparisons of the above measures between young vs. aged macaque retina. Together, these observations provide a foundation for the understanding of the innate immune system in the primate macula. They also reflect how microglial physiology and function may be adapted to the specializations in the macula and raise hypotheses on potential immune vulnerabilities that may occur there.

Methods

Isolation of retinal tissue

Eye tissue from three young female adult (4.2–5.5 years, equivalent to human age 13–17 years) and four middle-aged (16.8–18.2 years, equivalent to human age 50–55 years, using the general approximation of 3:1 ratio for human:rhesus age) female rhesus macaque (*Macaca mulatta*) primates was obtained from the Wisconsin National Primate Research Center of the University of Wisconsin-Madison. All experimental methods and techniques adhered to the Association for Research in Vision and Ophthalmology Statement for the Use of Animals in Ophthalmic and Vision Research and were approved by the University of Wisconsin-Madison animal care and use committee. The animals were euthanized by initial anesthesia with intramuscular injection of ketamine (10 mg/kg) followed by an overdose of intravenous pentobarbital starting at 50 mg/kg. The animals were enucleated promptly following euthanasia. The anterior segments of isolated globes were removed and remaining posterior segments were fixed in 4% paraformaldehyde at 4° C for 2 days and then stored in 0.1 M phosphate buffer at 4° C. For isolation of retinal tissue, posterior segments were visualized under a dissecting microscope and circular retinal tissue specimens obtained using a tissue punch (Acu-punch biopsy punch, Acuderm) at the following retinal locations: (1) fovea (3 mm-diameter punch centered on the fovea center), (2) outer macular region (2 mm-diameter punch with its center positioned 2.5mm temporal from the foveal center), and (3) peripheral extramacular region (2 mm-diameter punch with its center positioned 9–10mm from the foveal center in the temporal quadrant). Retinal tissue specimens were obtained from 8 eyes of 3 young and 4 middle-aged animals, one sample from each of the three retinal locations was obtained from each eye.

Immunohistochemical analysis

A subset of tissue specimens was embedded in 7% agarose (Sigma) and 100µm-thick retinal sections were prepared using a vibrating microtome (VT1000S, Leica). The remaining retinal tissue punches were processed as retinal flat-mounts. Immunohistochemical analyses were performed on flat-mounted and sectioned tissue with the following primary antibodies: rabbit anti-ionized calcium-binding adaptor molecule 1 (Iba1) Iba1 (Wako, #019-19741, 1:500), a protein specifically expressed by microglia among CNS cells in multiple species, including the non-human primate (Schmidt et al. 2016; Barkholt et al. 2012; Tonchev et al. 2003); and the cone-specific monoclonal antibody, 7G6, which recognizes cone arrestin in primates (a gift from Dr. Peter MacLeish, Morehouse School of Medicine, Atlanta, GA;

1:100)(Wikler et al. 1997; Zhang et al. 2003). Retinal tissue was also stained with 4',6-diamidino-2-phenylindole (DAPI; 1:1000; Invitrogen) to mark the retinal nuclear layers and with Isolectin-B4 (IB4) conjugated to AlexaFluor 568 (1:50, Life Technologies), to mark retinal blood vessels. Retinal sections were processed by blocking overnight in 0.1M phosphate-buffered saline (PBS) containing 7% normal goat serum, 0.5% Triton X-100 and 0.1% sodium azide. Sections were incubated in PBS with Triton-X containing primary antibodies and 2% normal goat serum at 4°C overnight, and washed in 1× PBS with Triton-X overnight. Samples were then incubated with secondary antibodies overnight at 4°C and washed in PBS with Triton-X overnight. Retinal flat-mount specimens were blocked similarly and incubated with primary antibody and 2% normal goat serum at 4°C for 12–14 days. Samples were rinsed overnight and incubated with secondary antibody at 4°C for 7 days before washing overnight in PBS with Triton-X.

Confocal imaging of retinal samples

Following immunolabeling, retinal tissue samples were mounted on glass slides and imaged using confocal microscopy. For retinal sections, multiplane z-series were collected using a 20× objective with each section spaced 1 μm apart to z-depths ranging from 48 to 85 μm (Zeiss LSM 700). For retinal flat-mounted specimens, multiplane z-series at 20× magnification ranging from the inner surface of the retina to the outer nuclear layer (z-step of 1–1.5 μm, total z-depth of 54 to 100 μm) were collected as overlapping imaging fields covering the entire retina punch specimen (Zeiss LSM 780, 880). These image stacks were subsequently processed using the Stitching function in the Zeiss software system (Version 11.0.3.190) to form a single stack of images subtending the whole specimen.

Image analysis

Microglia and cone cell densities were obtained by performing manual cell counts in 20× magnification multiplane z-series of flat-mounted retinal specimens using image processing software (ImageJ, NIH). Image analyses were performed within 3–4 regions of interest (or imaging fields) measuring 525 by 525 μm and extending across the thickness of the retina that were well-spaced across each retinal tissue punch specimen. Microglial counts were obtained separately in the ganglion cell layer (GCL), inner plexiform layer (IPL), and outer plexiform layer (OPL) of each imaging field. Three-dimensional morphological analyses of microglia were performed using computer-assisted segmentation of microglial processes (Filament Tracer module and the Convex Hull feature, Imaris software). Morphological parameters quantitated were: (1) prolate ellipticity (a measure of elongation in the bounding contour surface surrounding a single microglial dendritic field), (2) total number of branching points in a microglial dendritic field, (3) total dendritic process length in a microglial cell, and (4) mean volume occupied per cell (the 3-dimensional volume subtended by a single microglial dendritic field).

Statistical analysis

All data were analyzed using statistical software (GraphPad Prism Software, Version 6.0.1). A D'Agostino and Pearson normality test was used to analyze the distribution of all data sets. For two-way comparisons of data following a Gaussian distribution, independent data sets were analyzed with an unpaired two-tailed t-test. For 3-way comparisons, data were

analyzed with a 1-way ANOVA. Correlation analysis was performed by the computation of the Pearson correlation. A P-value < 0.05 was set as the basis for rejecting the null hypothesis. In all graphical representations, the heights of columns indicate means and error bars indicate standard error (SE).

Results

General distribution of microglia in the adult *rhesus macaque* primate retina

Posterior segments of three young and four middle-aged rhesus macaques were examined and retinal tissue samples corresponding to three retinal loci along the center-to-periphery axis were obtained and analyzed (Fig. 1A). Foveal retinal samples were obtained using a circular tissue punch of 3 mm-diameter centered on the foveal center; this enabled analysis of microglial distribution and morphology (1) in the foveal center within the foveal avascular zone (FAZ) and (2) in the vascularized parafoveal region (0.5–1.5mm from the foveal center). Outer macular retinal samples were obtained using a 2-mm diameter circular tissue punch positioned 2.5mm from the foveal center, while peripheral retinal samples were obtained using a 2-mm diameter circular tissue punch positioned 9–10mm from the foveal center in the temporal quadrant. Immunohistochemical analyses of retinal sections obtained from these three retinal loci demonstrated that microglia generally appeared as Iba1-immunoreactive cells with ramified morphologies that were distributed across the retina, with their processes concentrated in the plexiform layers (Fig. 1B,C). In the OPL, microglial processes were observed to be in close juxtaposition with the axonal termini of photoreceptors, as previously described in a study using Golgi staining techniques (Boycott and Hopkins 1981).

Distribution and morphology of retinal microglia in the foveal center

Immunohistochemical analysis of Iba1 labeling was used to evaluate the distribution and morphology of retinal microglia in the foveal center. In contrast to the dense array of microglia tiling the remainder of the retina, microglia in the foveal center were sparse, with the bottom of the foveal contour being largely devoid of microglial coverage (Fig. 2A). This relative “microglia-free” zone also corresponds to the center of the foveal avascular zone (FAZ) (Fig. 2B). Isolated microglial cells were found on the sides of the foveal slope in the region where centrifugally-directed inner processes of the foveal cones (i.e. the Fibers of Henle) make synaptic contact with bipolar cells (inset in Fig. 2A). These microglia showed large ramified morphologies with long axes that circumferentially encircle the foveal center, with processes distributed at the inner limit of the FAZ and the zone of initial photoreceptor-bipolar synaptic contact (Fig. 2A,B). In the vascularized parafoveal retina (at a distance 0.5–1.5mm from the foveal center), microglia at the level of the OPL demonstrated elongated, spindle-shaped morphologies that were aligned in a radial orientation relative to the foveal center (Fig. 2C). The location and orientation of the microglia in this area corresponded closely to that of the cone axons of the Fibers of Henle radiating from the central fovea. Microglia in the IPL in this location were also elongated in morphology but less so than those in the OPL. These features of microglial distribution and morphology in the foveal center were similar in young and aged retinas.

Microglial distribution in the young adult macaque retina relative to retinal position along the central-to-peripheral axis

As retinal microglia represent ramified cells that tile the horizontal plane of the retina via non-overlapping dendritic arbors, the local density of microglia reflects the amount of microglial “coverage” present at a particular retinal locus. Given the functions of microglia in innate immunity (Chen and Xu 2015) and in synapse maintenance (Wang et al. 2016), the local density of microglia may potentially relate to the amount of immune surveillance and/or trophic influence in that location. As the primate retina contains gradients in the distributions of various retinal cell types from fovea to periphery, which may relate to position-specific dispositions to retinal disease (Curcio 2001), we were interested to examine whether and how microglial density varies across the macaque retina. We analyzed microglia density in different retinal lamina (GCL, IPL, OPL) and compared them between three retinal locations, (1) the parafoveal region adjacent to the foveal avascular zone (hereafter referred to as the foveal region), (2) the outer macula, and (3) the periphery. Flat-mounted retinal samples were imaged with multi-plane confocal microscopy and the density of Iba1-immunopositive cells were computed for each layer and location (Fig. 3A). We found that microglial density was generally lower in the GCL layer relative to the other layers and did not vary significantly with retinal location (Fig. 3B). In the IPL and the OPL, microglial densities were significantly higher in the foveal region than in the macula or the peripheral retina. The general trend in the changes in microglial density with retinal position corresponded to that of cone density (Fig. 3C)(Curcio et al. 1987); indeed microglia demonstrated multiple physical contacts between their processes and the ends of cone pedicles in the OPL (Fig. 3D), suggestive of a specialized interaction between these two cell types. We also found that the local microglia density in the OPL and IPL correlated well to the local cone density across retinal locations (Fig. 3E), indicating that the patterning of microglial distribution in the primate retina may be related to the graded distribution of retinal neurons, particularly those in the cone pathway (e.g. cone bipolar cells).

Microglial morphology in the young adult macaque retina relative to retinal position along the central-to-peripheral axis

Microglia cells demonstrate ramified morphologies that consist of dynamically moving processes that have been hypothesized to play roles in synaptic contact, phagocytosis of pathogens and debris, and delivery of trophic and inflammatory molecules (Gomez-Nicola and Perry 2015). As such, the features of microglial morphology can be shaped by their local environment and also reflect their physiological functions that exert on nearby cells (Walker et al. 2014). To investigate this, we examined whether microglial morphologies varied as a function of retinal position in the macaque retina. Following multi-plane confocal imaging of Iba1+ microglia in retinal flat-mounts, we performed quantitative 3-dimensional morphometric analyses of individual microglial cells in the fovea, macular, and peripheral regions using Imaris, an image analysis software (Fig. 4A). Individual cells were segmented and four morphometric measurements were quantified and compared: (1) prolate ellipticity, which provides a measure of elongation of the bounding ellipsoid surrounding the dendritic arbor of a cell, (2) number of branch points in the dendritic arbor of a single cell, (3) the total length of dendritic process of a single cell, and (4) the volume of the dendritic arbor of the cell, quantified as the volume of the convex envelope or hull containing the entire

dendritic arbor. These measures reflect the geometry of the cell and the ability of the cell to interact with its environment via its processes. As described earlier, these quantitative measures demonstrated that microglia in OPL of the fovea were considerably more elongated than in the macula and periphery, where the cells were more symmetrically oriented (Fig. 4B). Microglial dendritic arbors in the macula had significantly higher branch points (Fig. 4C), dendritic lengths (Fig. 4D), and volume (Fig. 4E) than those in the other two locations. In the IPL, foveal microglia were less elongated than in the OPL, but IPL macular microglia, like those in the OPL, similarly tended to have higher branch points, dendritic lengths, and volume (Supplementary Fig. 1), although the differences between locations were smaller than those found for OPL microglia. This data indicated that microglia in the macula had a greater potential ability to contact and interact with their environment relative to those in the periphery, where microglia were found in fewer numbers and were morphologically smaller and less complex.

Age-related changes in the distribution and morphology of microglia in the primate retina

To further understand the potential contribution of retinal microglia to age-related changes in the macula, including the increased vulnerability of the aging macula to degeneration such as that occurring in age-related macular degeneration (AMD), we examined how microglia in the primate retina demonstrated alterations with aging. We compared the densities of retinal microglia in the GCL, IPL and OPL at each of the 3 retinal locations (fovea, macula, periphery) between young (4.2–5.5 years) and aged (16.8–18.2 years) macaques (Fig. 5A,B). In the GCL, microglial densities tended to be slightly higher in the aged retina at all 3 retinal locations but these differences did not reach statistical significance. In the IPL and OPL, microglial densities in the fovea and macula, but not in the peripheral retina, were significantly higher in the aged retina relative to the young retina. This increase in microglial density with age was not mirrored by an increase in cone density in the corresponding location (Fig. 5C). However, the correlations between IPL/OPL microglial density and cone density remained present in the aged retina (Fig. 5D).

In contrast to age-related changes in distribution, measures of microglia morphology did not demonstrate broad and significant changes as a function of age. In the OPL of the aged retina, microglial morphometric measures of ellipticity (Fig. 6A), branch point number (Fig. 6B), dendritic length (Fig. 6C), and dendritic volume (Fig. 6D) demonstrated the same trends with retinal position as found in the OPL of the young retina, and did not demonstrate significant differences when compared with those in the young retina. Similar findings were also obtained in comparisons of IPL microglia in the young vs. aged retina (Supplementary Fig. 2).

Discussion

Recent studies in rodent model systems have uncovered new functional significant roles for retinal microglia in: (1) the constitutive maintenance of retinal synaptic structure and function (Wang et al. 2016), (2) the regulation of the magnitude of inflammatory responses (Wang et al. 2014), and (3) the pathogenesis and progression of retinal diseases (Karlstetter et al. 2015). How these findings relate to microglia in the primate retina, particularly with

respect to the macula, the locus of a number of retinal diseases, is not well understood. In early studies of microglia in the macaque retina which include those performed by Vrabec (Vrabec 1970) using a silver carbonate labeling technique, and by Boycott and Hopkins (Boycott and Hopkins 1981) using Golgi-impregnated retinal whole mounts, qualitative descriptions were provided of microglia as uniformly-spaced ramified cells positioned in the GCL, IPL, and OPL, and whose processes extend into close proximity to synaptic structures. Subsequent immunohistochemical studies performed in the adult human retina show that microglia there demonstrate similar general morphologies and distributions as those in the macaque retina and express leukocyte antigens such as CD45, major histocompatibility complex class II (MHC-II) (Penfold et al. 1991; Penfold et al. 1993) and class I (MHC-I) (Provis et al. 1995). However, comparative analyses of microglia in the primate retina using confocal microscopy and 3-dimensional morphometry across retinal position and organismal age have not been previously performed.

In our study, we observed that although microglia provide coverage to nearly all positions in the horizontal plane of the retina, the foveal center is interestingly devoid of significant microglial coverage, an observation also noted in previous descriptions of microglia in the human fovea (Diaz-Araya et al. 1995; Penfold et al. 1991). Studies of foveal ontogeny have suggested that as inner retinal cells undergo centrifugal migration during the formation of the foveal depression (Hendrickson and Yuodelis 1984), microglia may also be concurrently displaced from this central location. This particular feature indicates that unlike the remainder of the retina, there may not be a constitutive requirement for microglia at the central fovea. The absence of synapses and retinal vasculature at this locus may exempt this locus from a need for microglia-mediated synapse maintenance and for immune surveillance of materials entering the retina from the retinal vasculature. How this absence of retinal microglia may be significant to immune function or to the emergence of retinal pathology in this locus is unclear and awaits the detailed characterization of microglia in histopathological specimens of foveal disease.

In the macaque macula, the association between the presence of microglia and the presence of retinal vasculature and synapses was clearly observed at the border of the foveal avascular zone (FAZ), which is close to the zone where the most central synapses between cones and bipolar cells are found (i.e. where the Fibers of Henle make synaptic contact). In this region, comprehensive coverage of the retina by microglia commences and in this region, microglia were observed to encircle the edge of the FAZ and the concentric ring of initial cone-bipolar synapses, coming into close contact with retinal vessels and synapses via their processes, as described previously in earlier studies (Boycott and Hopkins 1981; West 1978). The highest densities of microglia in the macaque retina were found in the vascularized parafoveal region (0.5–1.5mm from the foveal center) in the OPL and IPL; in the IPL, the microglial density in the parafovea was nearly twice that in the peripheral retina. These gradients of microglial density may relate to the greater synaptic densities in the plexiform layers in the more central regions of the retina – the gradient of microglia density from center to periphery correlated well to the gradient of cone density along the same axis. In our previous work in the mouse retina, we found that synaptic degeneration and loss of synaptic transmission occurred upon microglia depletion (Wang et al. 2016), indicating a requirement of microglia for healthy synaptic structure and function. The mechanism underlying this

microglia-mediated synapse maintenance is thought to involve the local delivery of neurotrophic factors, such as brain-derived growth factor (BDNF), from microglia to synapses (Parkhurst et al. 2013). Indeed, the dynamic movements of microglia processes have been described to facilitate repeated synaptic contact in an activity dependent manner (Tremblay et al. 2010; Wake et al. 2009). The greater requirement for microglia-derived trophic factors and for dynamic microglia-synapse contact in synapse-rich regions may therefore translate to a need to maintain higher microglial numbers locally. However what factors and mechanisms set up and maintain the patterning of microglial distribution in the retina is unknown and are under current investigation in our laboratory.

In addition to microglial density, the morphology of individual microglial cells appears to demonstrate regional specialization in the macaque retina. The morphological features of microglia in the context of injury or disease have been associated with physiological processes such as activation, migration, surveillance, or phagocytosis (Walker et al. 2014). The functional significance of varying microglial morphology in the healthy CNS is not as clear but multiple studies have found that changes in neuronal activity can modulate microglial morphology (Fontainhas et al. 2011; Nimmerjahn et al. 2005; Li et al. 2012). As such, microglial morphology may potentially be patterned to subserve differing physiological requirements in the different local areas of the retina. We noted that microglia in the outer macula of the macaque demonstrated the largest dendritic arbors with the highest degree of complexity. This may be a reflection of a higher physiological and neuronal activity of the macula relative to that in the periphery, requiring a higher coverage by microglial processes. The foveal region, owing to space constraints may not be able to accommodate large microglial dendritic arbors and so compensates by having a larger number of microglia with smaller arbors. It is possible that the morphologic specialization of macular microglia may influence microglial responses to injury, and may thus confer to the macula a different immune responsiveness that may be influential to injury outcome.

We found in this study that while microglial morphologies in each retinal locus do not change significantly with aging, the density of microglia in the fovea and macular regions, but not the peripheral region, increases as a function of age. The increase in microglia numbers with aging has been documented in a number of CNS regions (Hefendehl et al. 2014; Tremblay et al. 2012); in a previous study from our laboratory examining aging changes in microglia in the mouse retina (Damani et al. 2011), we found that increasing age was correlated with (1) increased microglial density in the IPL and OPL, (2) decreased microglial arbor size and ramification, (3) decreased dynamic process motility on live cell imaging. In comparison, the aging primate retina demonstrated a similar increase in retinal microglia density that was significant in the macula but not in the peripheral retina. The reasons for increasing microglial density with aging is unclear; it has been hypothesized that this increase may arise from altered homeostasis of microglial numbers, from a physiological compensation for functional declines in individual aging microglia (Wong 2013), or from intrinsic changes in microglial gene expression profiles (Ma et al. 2013). The observed increase in microglial density in the aging macula, together with the more activated status of senescent microglia (Norden et al. 2015), has the potential to place the macula at a greater risk for exaggerated and dysregulated immune responses and in so doing, predispose the macula to neuroinflammatory disease, such as age-related macular degeneration (AMD)

(Ma and Wong 2016; Chen and Xu 2015; Karlstetter and Langmann 2014). We did not however observe statistically significant changes in the morphological parameters of microglia in the primate retina that we had previously found in the mouse retina (Damani et al. 2011). The reasons for these differences are unclear; they may be related to differences between microglia in different CNS compartments or to the differences in the neural environment in each case. It is possible that morphological change in microglia is a late phenomenon in microglia senescence in the primate retina which only becomes apparent at ages older than the ones studied here. Also, as we have limited our evaluation to female animals to limit the variables in our analysis, whether these aging trends hold in male animals will be a topic for future study.

In conclusion, microglial distribution and morphology in the primate retina, demonstrates significant diversity and regional specializations not observed in rodent models. These specializations, which are found in a graded fashion along the center-to-periphery axis, may be secondary to functional specializations in the macula and may also be relevant to the vulnerability of the macula to neuroinflammatory disease. The graded increase in microglial density in the macula relative to the periphery are augmented with aging, and may further increase the predilection for neuroinflammation in the aged macula. Further studies into age-related alterations of the immune system within the primate retina have the potential to uncover pathogenic mechanisms relevant to diseases such as AMD.

Supplementary Material

Refer to Web version on PubMed Central for supplementary material.

Acknowledgments

The authors are grateful to Dr. Peter MacLeish, Morehouse School of Medicine, Atlanta, GA, for the generous gift of the 7G6 antibody and to Dr. Paul Kaufman, Department of Ophthalmology & Visual Sciences, University of Wisconsin-Madison, for his guidance and encouragement. This work is supported by the National Eye Institute Intramural Research Program. J.S. is supported by the NIH Medical Research Scholars Program, a public-private partnership supported jointly by the NIH and generous contributions to the Foundation for the NIH from the Doris Duke Charitable Foundation, The American Association for Dental Research, The Howard Hughes Medical Institute, and the Colgate-Palmolive Company, as well as other private donors. T.M.N. is supported by NIH NEI Core Grant P30 EY016665, Research to Prevent Blindness, the Wisconsin National Primate Research Center P51RR000167/P51OD011106, and the Retina Research Foundation Catherine and Latimer Murfee chair.

References

- Boycott BB, Hopkins JM. Microglia in the retina of monkey and other mammals: its distinction from other types of glia and horizontal cells. *Neuroscience*. 1981; 6(4):679–688. [PubMed: 6165924]
- Chen M, Xu H. Parainflammation, chronic inflammation, and age-related macular degeneration. *Journal of leukocyte biology*. 2015; 98(5):713–725. DOI: 10.1189/jlb.3RI0615-239R [PubMed: 26292978]
- Curcio CA. Photoreceptor topography in ageing and age-related maculopathy. *Eye*. 2001; 15(Pt 3): 376–383. DOI: 10.1038/eye.2001.140 [PubMed: 11450761]
- Curcio CA, Sloan KR Jr, Packer O, Hendrickson AE, Kalina RE. Distribution of cones in human and monkey retina: individual variability and radial asymmetry. *Science*. 1987; 236(4801):579–582. [PubMed: 3576186]

- Damani MR, Zhao L, Fontainhas AM, Amaral J, Fariss RN, Wong WT. Age-related alterations in the dynamic behavior of microglia. *Aging cell*. 2011; 10(2):263–276. DOI: 10.1111/j.1474-9726.2010.00660.x [PubMed: 21108733]
- Diaz-Araya CM, Provis JM, Penfold PL, Billson FA. Development of microglial topography in human retina. *The Journal of comparative neurology*. 1995; 363(1):53–68. DOI: 10.1002/cne.903630106 [PubMed: 8682937]
- Eyo UB, Wu LJ. Bidirectional microglia-neuron communication in the healthy brain. *Neural plasticity*. 2013; 2013:456857. doi: 10.1155/2013/456857 [PubMed: 24078884]
- Fontainhas AM, Wang M, Liang KJ, Chen S, Mettu P, Damani M, Fariss RN, Li W, Wong WT. Microglial morphology and dynamic behavior is regulated by ionotropic glutamatergic and GABAergic neurotransmission. *PloS one*. 2011; 6(1):e15973. doi: 10.1371/journal.pone.0015973 [PubMed: 21283568]
- Frost JL, Schafer DP. Microglia: Architects of the Developing Nervous System. *Trends in cell biology*. 2016; doi: 10.1016/j.tcb.2016.02.006
- Gomez-Nicola D, Perry VH. Microglial dynamics and role in the healthy and diseased brain: a paradigm of functional plasticity. *The Neuroscientist : a review journal bringing neurobiology, neurology and psychiatry*. 2015; 21(2):169–184. DOI: 10.1177/1073858414530512
- Hefendehl JK, Neher JJ, Suhs RB, Kohsaka S, Skodras A, Jucker M. Homeostatic and injury-induced microglia behavior in the aging brain. *Aging cell*. 2014; 13(1):60–69. DOI: 10.1111/ace1.12149 [PubMed: 23953759]
- Hendrickson AE, Yuodelis C. The morphological development of the human fovea. *Ophthalmology*. 1984; 91(6):603–612. [PubMed: 6462623]
- Hristovska I, Pascual O. Deciphering Resting Microglial Morphology and Process Motility from a Synaptic Prospect. *Frontiers in integrative neuroscience*. 2015; 9:73. doi: 10.3389/fnint.2015.00073 [PubMed: 26834588]
- Karlstetter M, Langmann T. Microglia in the aging retina. *Advances in experimental medicine and biology*. 2014; 801:207–212. DOI: 10.1007/978-1-4614-3209-8_27 [PubMed: 24664700]
- Karlstetter M, Scholz R, Rutar M, Wong WT, Provis JM, Langmann T. Retinal microglia: just bystander or target for therapy? *Progress in retinal and eye research*. 2015; 45:30–57. DOI: 10.1016/j.preteyeres.2014.11.004 [PubMed: 25476242]
- Lee JE, Liang KJ, Fariss RN, Wong WT. Ex vivo dynamic imaging of retinal microglia using time-lapse confocal microscopy. *Investigative ophthalmology & visual science*. 2008; 49(9):4169–4176. DOI: 10.1167/iovs.08-2076 [PubMed: 18487378]
- Li L, Eter N, Heiduschka P. The microglia in healthy and diseased retina. *Experimental eye research*. 2015; 136:116–130. DOI: 10.1016/j.exer.2015.04.020 [PubMed: 25952657]
- Li Y, Du XF, Liu CS, Wen ZL, Du JL. Reciprocal regulation between resting microglial dynamics and neuronal activity in vivo. *Developmental cell*. 2012; 23(6):1189–1202. DOI: 10.1016/j.devcel.2012.10.027 [PubMed: 23201120]
- Ma W, Cojocaru R, Gotoh N, Gieser L, Villasmil R, Cogliati T, Swaroop A, Wong WT. Gene expression changes in aging retinal microglia: relationship to microglial support functions and regulation of activation. *Neurobiology of aging*. 2013; 34(10):2310–2321. DOI: 10.1016/j.neurobiolaging.2013.03.022 [PubMed: 23608111]
- Ma W, Wong WT. Aging Changes in Retinal Microglia and their Relevance to Age-related Retinal Disease. *Advances in experimental medicine and biology*. 2016; 854:73–78. DOI: 10.1007/978-3-319-17121-0_11 [PubMed: 26427396]
- Madeira MH, Boia R, Santos PF, Ambrosio AF, Santiago AR. Contribution of microglia-mediated neuroinflammation to retinal degenerative diseases. *Mediators of inflammation*. 2015; 2015:673090. doi: 10.1155/2015/673090 [PubMed: 25873768]
- McGeer PL, McGeer EG. Targeting microglia for the treatment of Alzheimer's disease. *Expert opinion on therapeutic targets*. 2015; 19(4):497–506. DOI: 10.1517/14728222.2014.988707 [PubMed: 25435348]
- Ng TF, Streilein JW. Light-induced migration of retinal microglia into the subretinal space. *Investigative ophthalmology & visual science*. 2001; 42(13):3301–3310. [PubMed: 11726637]

- Nimmerjahn A, Kirchhoff F, Helmchen F. Resting microglial cells are highly dynamic surveillants of brain parenchyma in vivo. *Science*. 2005; 308(5726):1314–1318. DOI: 10.1126/science.1110647 [PubMed: 15831717]
- Norden DM, Muccigrosso MM, Godbout JP. Microglial priming and enhanced reactivity to secondary insult in aging, and traumatic CNS injury, and neurodegenerative disease. *Neuropharmacology*. 2015; 96(Pt A):29–41. DOI: 10.1016/j.neuropharm.2014.10.028 [PubMed: 25445485]
- Parkhurst CN, Yang G, Ninan I, Savas JN, Yates JR 3rd, Lafaille JJ, Hempstead BL, Littman DR, Gan WB. Microglia promote learning-dependent synapse formation through brain-derived neurotrophic factor. *Cell*. 2013; 155(7):1596–1609. DOI: 10.1016/j.cell.2013.11.030 [PubMed: 24360280]
- Penfold PL, Madigan MC, Provis JM. Antibodies to human leucocyte antigens indicate subpopulations of microglia in human retina. *Visual neuroscience*. 1991; 7(4):383–388. [PubMed: 1751423]
- Penfold PL, Provis JM, Liew SC. Human retinal microglia express phenotypic characteristics in common with dendritic antigen-presenting cells. *Journal of neuroimmunology*. 1993; 45(1–2): 183–191. [PubMed: 8392519]
- Perry VH, Holmes C. Microglial priming in neurodegenerative disease. *Nature reviews Neurology*. 2014; 10(4):217–224. DOI: 10.1038/nrneurol.2014.38 [PubMed: 24638131]
- Provis JM, Penfold PL, Edwards AJ, van Driel D. Human retinal microglia: expression of immune markers and relationship to the glia limitans. *Glia*. 1995; 14(4):243–256. DOI: 10.1002/glia.440140402 [PubMed: 8530182]
- Tay TL, Savage J, Hui CW, Bisht K, Tremblay ME. Microglia across the lifespan: from origin to function in brain development, plasticity and cognition. *The Journal of physiology*. 2016; doi: 10.1113/JP272134
- Thanos S. Sick photoreceptors attract activated microglia from the ganglion cell layer: a model to study the inflammatory cascades in rats with inherited retinal dystrophy. *Brain research*. 1992; 588(1):21–28. [PubMed: 1393569]
- Tremblay ME, Lowery RL, Majewska AK. Microglial interactions with synapses are modulated by visual experience. *PLoS biology*. 2010; 8(11):e1000527. doi: 10.1371/journal.pbio.1000527 [PubMed: 21072242]
- Tremblay ME, Zettel ML, Ison JR, Allen PD, Majewska AK. Effects of aging and sensory loss on glial cells in mouse visual and auditory cortices. *Glia*. 2012; 60(4):541–558. DOI: 10.1002/glia.22287 [PubMed: 22223464]
- von Bernhardt R, Eugenin-von Bernhardt L, Eugenin J. Microglial cell dysregulation in brain aging and neurodegeneration. *Frontiers in aging neuroscience*. 2015; 7:124. doi: 10.3389/fnagi.2015.00124 [PubMed: 26257642]
- Vrabec F. Microglia in the monkey and rabbit retina. *Journal of neuropathology and experimental neurology*. 1970; 29(2):217–224. [PubMed: 4190979]
- Wake H, Moorhouse AJ, Jinno S, Kohsaka S, Nabekura J. Resting microglia directly monitor the functional state of synapses in vivo and determine the fate of ischemic terminals. *The Journal of neuroscience : the official journal of the Society for Neuroscience*. 2009; 29(13):3974–3980. DOI: 10.1523/JNEUROSCI.4363-08.2009 [PubMed: 19339593]
- Walker FR, Beynon SB, Jones KA, Zhao Z, Kongsui R, Cairns M, Nilsson M. Dynamic structural remodelling of microglia in health and disease: a review of the models, the signals and the mechanisms. *Brain, behavior, and immunity*. 2014; 37:1–14. DOI: 10.1016/j.bbi.2013.12.010
- Wang M, Wang X, Zhao L, Ma W, Rodriguez IR, Fariss RN, Wong WT. Macrogliia-microglia interactions via TSPO signaling regulates microglial activation in the mouse retina. *The Journal of neuroscience : the official journal of the Society for Neuroscience*. 2014; 34(10):3793–3806. DOI: 10.1523/JNEUROSCI.3153-13.2014 [PubMed: 24599476]
- Wang X, Zhao L, Zhang J, Fariss RN, Ma W, Kretschmer F, Wang M, Qian HH, Badea TC, Diamond JS, Gan WB, Roger JE, Wong WT. Requirement for Microglia for the Maintenance of Synaptic Function and Integrity in the Mature Retina. *The Journal of neuroscience : the official journal of the Society for Neuroscience*. 2016; 36(9):2827–2842. DOI: 10.1523/JNEUROSCI.3575-15.2016 [PubMed: 26937019]
- West RW. Bipolar and horizontal cells of the gray squirrel retina: Golgi morphology and receptor connections. *Vision research*. 1978; 18(2):129–136. [PubMed: 664282]

- Wikler KC, Rakic P, Bhattacharyya N, Macleish PR. Early emergence of photoreceptor mosaicism in the primate retina revealed by a novel cone-specific monoclonal antibody. *The Journal of comparative neurology*. 1997; 377(4):500–508. [PubMed: 9007188]
- Wong WT. Microglial aging in the healthy CNS: phenotypes, drivers, and rejuvenation. *Frontiers in cellular neuroscience*. 2013; 7:22.doi: 10.3389/fncel.2013.00022 [PubMed: 23493481]
- Zhang H, Cuenca N, Ivanova T, Church-Kopish J, Frederick JM, MacLeish PR, Baehr W. Identification and light-dependent translocation of a cone-specific antigen, cone arrestin, recognized by monoclonal antibody 7G6. *Investigative ophthalmology & visual science*. 2003; 44(7):2858–2867. [PubMed: 12824223]
- Zhao L, Zabel MK, Wang X, Ma W, Shah P, Fariss RN, Qian H, Parkhurst CN, Gan WB, Wong WT. Microglial phagocytosis of living photoreceptors contributes to inherited retinal degeneration. *EMBO molecular medicine*. 2015; 7(9):1179–1197. DOI: 10.15252/emmm.201505298 [PubMed: 26139610]

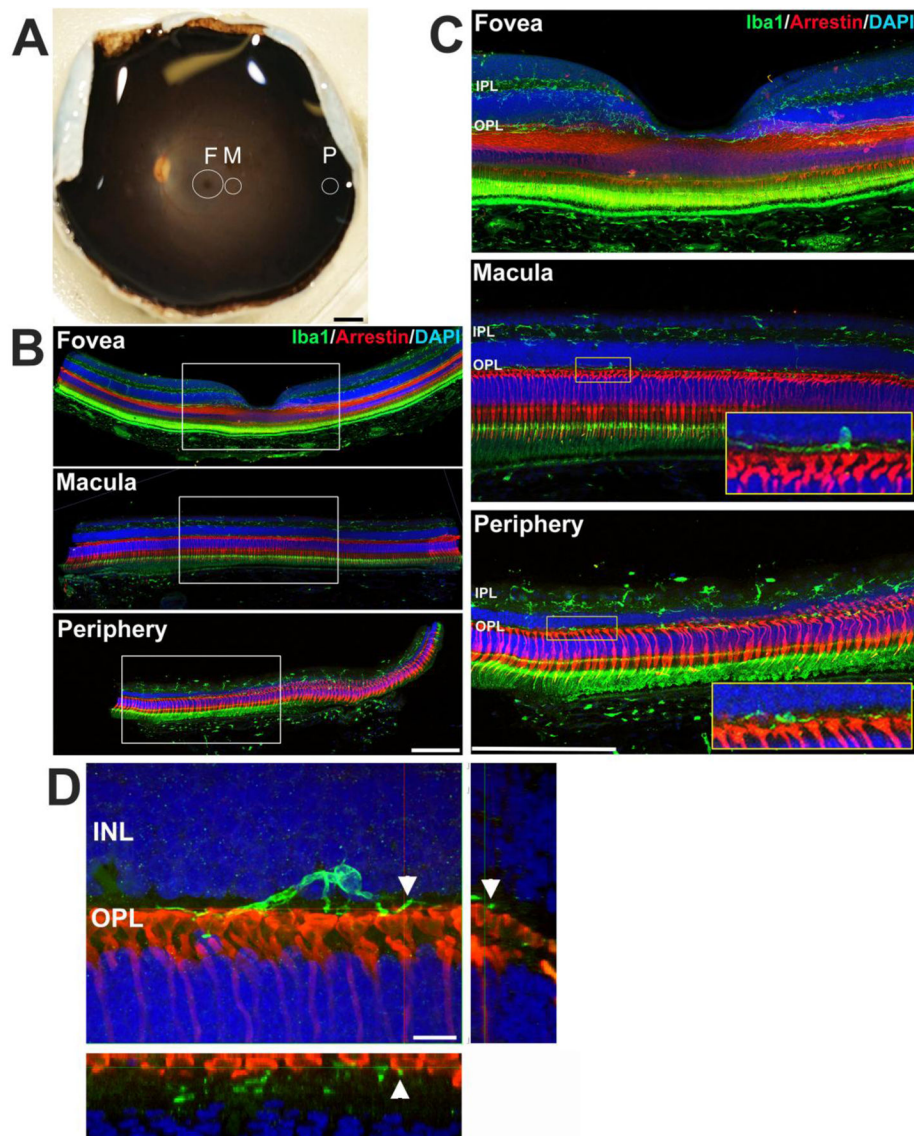


Figure 1. Regional analysis of microglia in the adult rhesus macaque (*Macaca mulatta*) primate retina

(A) Photograph of the posterior eye-cup from a young adult animal, illustrating the retinal topographical regions analyzed. Circular tissue punches were made in three retinal regions: (1) fovea (F, 3 mm-diameter punch centered on the foveal center), (2) outer macular region (M, 2 mm-diameter punch with its center positioned 2.5mm from the foveal center), and (3) peripheral extramacular region (P, 2 mm-diameter punch with its center positioned 9–10mm from the foveal center). Retinal tissue in each region was subjected to histological analysis. (B,C) Immunohistological analyses in retinal sections from each of the 3 regions demonstrated the distribution of retinal microglia in separate retina lamina. Panel (C) shows high-magnification views of the insets in (B). Retinal microglia, labeled with Iba1 (*green*), are primarily distributed in the inner and outer plexiform layers (IPL, OPL) (nuclear layers labeled with DAPI, *blue*). Microglia in the OPL are juxtaposed closely with the axon termini of photoreceptor cones (labeled with cone arrestin, *red*; insets in C). The signals in the

photoreceptor outer segments and retinal pigment epithelial cell layer arise from endogenous fluorescence. Iba1 immunopositivity in the choroid labels resident choroidal macrophages. **(D)** High magnification view of a microglial cells in the macula demonstrating point contact between microglial processes and cone photoreceptor pedicles (*arrowheads*); insets show orthogonal views of microglia-pedicle contact. Scale bars = 2.5mm in (A), 200 μm in (B), 200 μm in (C), 10 μm in (D)

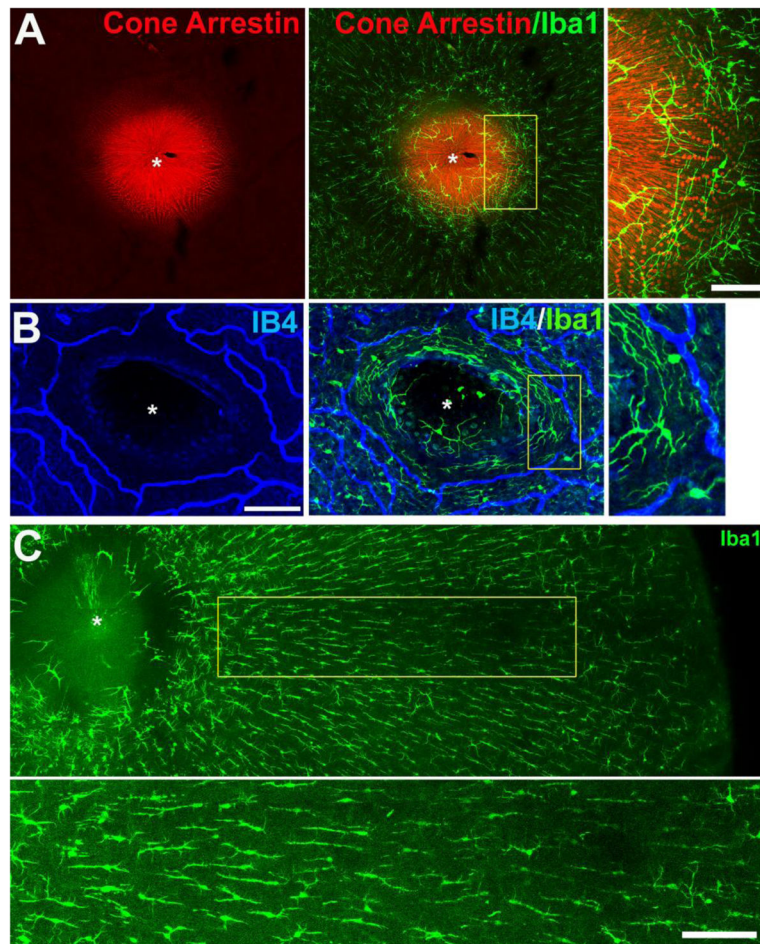


Figure 2. Morphology and distribution of microglia in the macaque foveal retina

(A) Confocal micrograph of a flat-mounted retina from the fovea region of a 14.7-year old female macaque, showing the distribution of cone outer segments and the fiber layer of Henle (labeled with cone arrestin, *red*), juxtaposed with microglia in the foveal region (labeled with Iba1, *green*). While microglia are found at all retinal positions from center to periphery, they are sparse in the foveal center (marked with *). Inset shows a high-magnification view of perifoveal microglia which demonstrated large dendritic arbors that have a circumferential orientation around the foveal center. Scale bar = 50 μm . (B) Confocal micrograph of another flat-mounted retina from the fovea of a 4.2-year old female macaque in which the retinal vasculature had been labeled with isolectin B4 (IB4, *blue*). Microglia labeled with Iba1 (*green*) were found in a circumferential orientation on the margin of the foveal avascular zone. Scale bar = 100 μm . (C) Low-magnification view of the microglia in the outer plexiform layer (OPL) of the foveal region, demonstrating a morphological transition from arbors with a circumferential orientation near the foveal center to those with radially-oriented, spindle-shaped morphologies further away from the foveal center (inset shows a high-magnification view below) Scale bar = 200 μm .

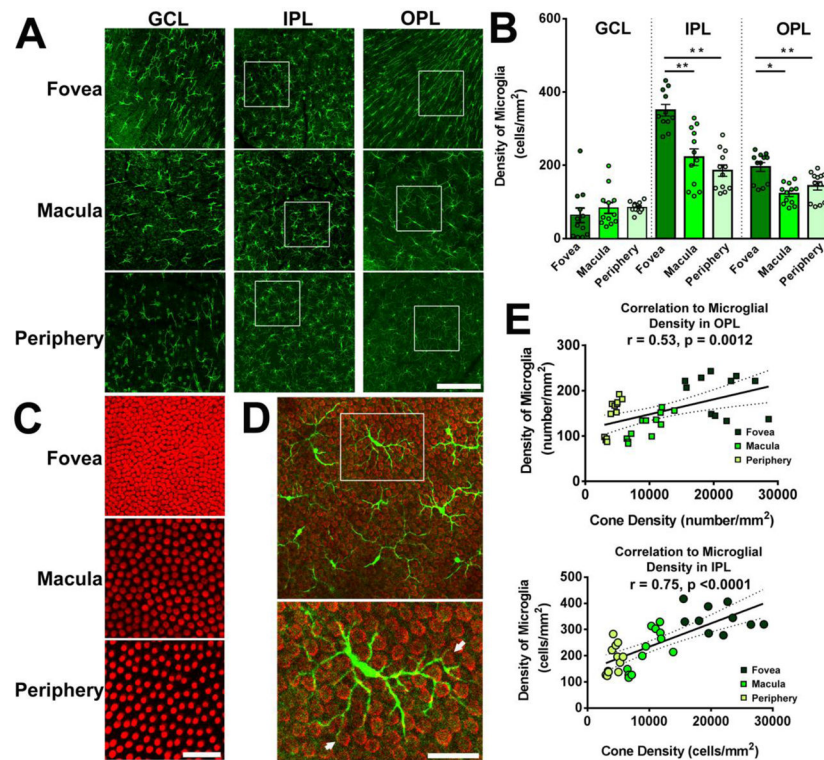


Figure 3. Microglial distribution in the young adult macaque retina demonstrates regional specialization with regards to retinal position

(A) Confocal micrographs showing Iba1-labeled retinal microglia in each of the specified retinal regions (fovea, macula, periphery) of young adult macaques (4.2–5.5 years) at the level of the ganglion cell layer (GCL), inner plexiform layer (IPL), and outer plexiform layer (OPL). Analysis in the foveal region was conducted approximately 0.5–1.5 mm from the foveal center. Scale bar = 100 μ m. (B) Quantification of microglial density in each retinal layer with respect to retinal location. While microglia densities in the GCL were comparable across retinal regions, those in the IPL and OPL were significantly greater in the foveal region, relative to the macular and peripheral locations, indicating a higher concentration of microglia with greater proximity to the foveal center (** indicates $P < 0.0001$, * indicates $P < 0.005$, 1-way ANOVA, $n = 3$ –4 imaging fields analyzed per retinal location from each of 3 animals). (C) Confocal micrographs showing cone arrestin-labeled cone outer segments, showing the progression of cone densities with retinal position. Scale bar = 100 μ m. (D) Superposition of Iba1+ microglia (green) in the OPL and cone arrestin-labeled cone pedicles (red) in the macula area demonstrate close interaction between microglial processes and cone pedicles (arrows in lower panel, from inset at higher magnification). Scale bar = 30 μ m. (E) Plots of cone densities in foveal, macular, and peripheral locations vs. microglial densities in the OPL (upper panel) and in the IPL (lower panel), showing correlations between microglial density and cone density across retinal positions (Pearson r and p value computed for correlations between cone density and microglial density counted from $n = 12$ imaging fields in 3 young animals).

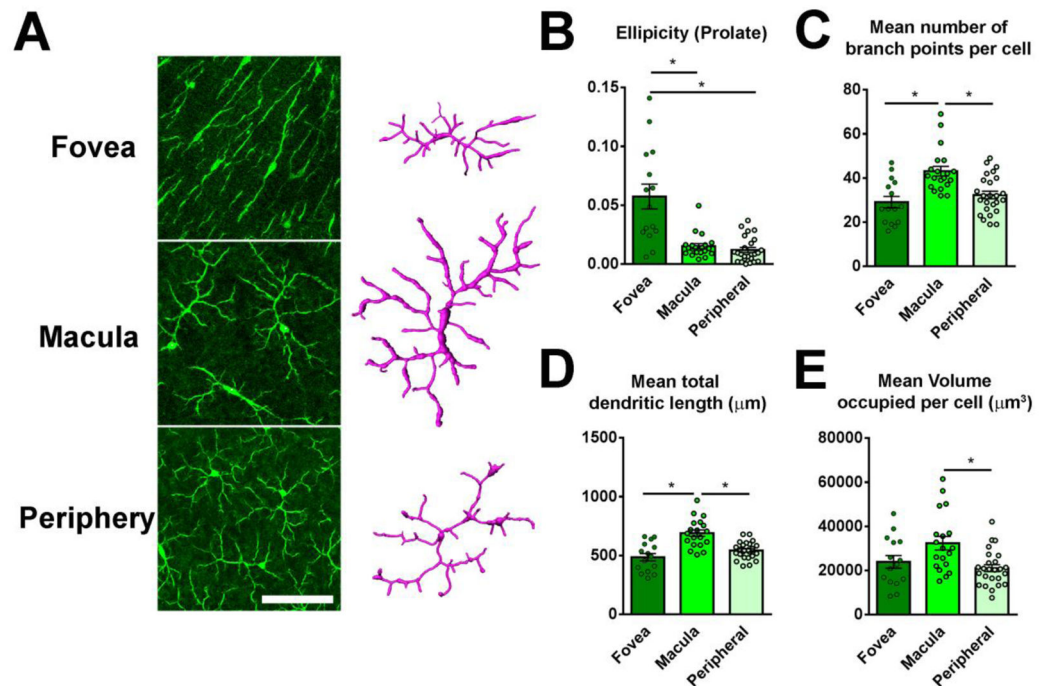


Figure 4. Microglial morphology in the outer plexiform layer (OPL) of the young adult macaque retina demonstrates regional specialization with regards to retinal position

(A) Confocal micrographs of microglia in the OPL in the areas of the fovea, macula, and periphery. Scale bar = 200 μm . Representative 3-dimensional computer-assisted reconstructions of the morphology of individual microglia cells were made in the three retinal areas for analysis; representative examples are shown. (B) Results of morphological analyses of microglia in the OPL demonstrate that the dendritic arbors of foveal microglia were more elongated, and have significantly greater ellipticity measures (elongation along the long axis), while macula and peripheral microglia in the OPL were minimally elongated and generally symmetric. (C) Macular OPL microglia, relative to peripheral OPL microglia demonstrated significantly greater mean number of branch points (D), mean total dendritic length (E), and greater mean volume per cell (F), indicating a regional specialization in terms of morphology. (* indicate $P < 0.05$, 1-way ANOVA, Kruskal-Wallis test, 5–10 microglia analyzed in each retinal location from each of 3 young animals).

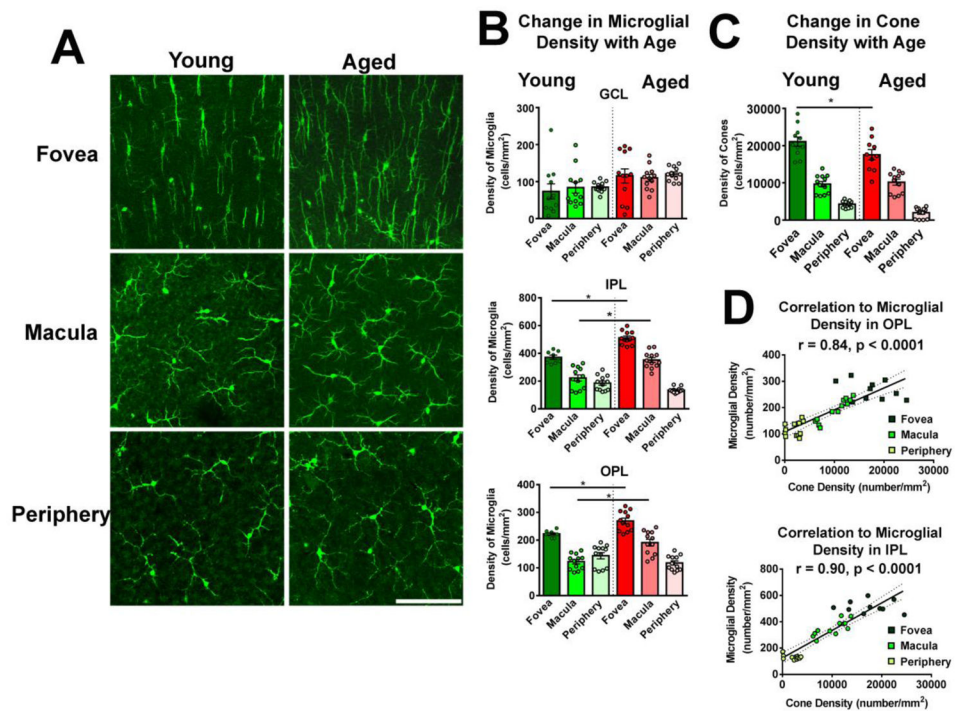


Figure 5. Microglial density increases in the aged macaque fovea and macula as a function of aging

(A) Representative confocal micrographs comparing microglia in the OPL between young and aged retinas in the areas of the fovea, macula, and periphery. Scale bar = 100 μm . (B) Microglial density was measured in aged (16.8–18.2 years) *Macaca mulatta* primate monkeys ($n = 3$) in foveal, macular, and peripheral retinal locations and compared with those measures in young (4.2–5.5 years) macaques. Comparison of microglial densities in equivalent retinal locations demonstrated generally higher microglial densities in the aged vs. the young retina. Significant age-related differences were found in the IPL and OPL layers in foveal and macular locations. (C) Comparison of cone photoreceptor densities shows general equivalence between young vs. aged animals, with the exception of slightly lower cone density in the aged fovea (A, B: * indicate $P < 0.05$, 1-way ANOVA, $n = 12$ imaging fields each in 3 young and 3 aged adult animals). (D) Plots of cone densities in foveal, macular, and peripheral locations vs. microglial densities in the OPL (*upper* panel) and in the IPL (*lower* panel) in aged animals show similar correlations as previously observed in young animals (Pearson r and p value computed for correlations between cone density and microglial density, $n = 34$ imaging fields in 3 aged animals).

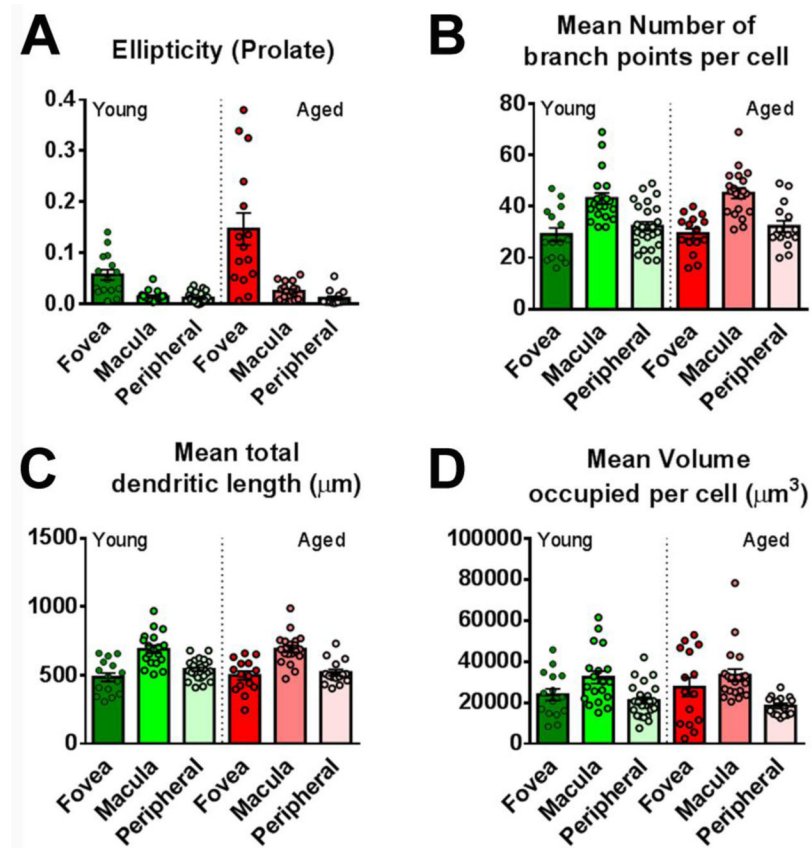


Figure 6. Measures of microglial morphologies in the OPL are unchanged with aging in the macaque retina

Mean measures of morphological features of OPL microglia were compared between young and aged retinas in terms of (A) ellipticity, (B) mean number of branch points, (C) mean total dendritic length, and (D) mean volume. Microglia in the aged OPL demonstrated the same regional specializations as did microglia in the young OPL, and young-vs-aged comparisons between matched areas did not reveal any significant differences for all parameters (* indicate $P < 0.05$, 1-way ANOVA, Kruskal-Wallis test, 5–10 microglia analyzed in each retinal location from each of 3 young and 3 aged animals).